A Random Finite Set Approach to Bayesian SLAM

John Mullane, Ba-Ngu Vo, Martin D. Adams, Ba-Tuong Vo

***Abstract*—This paper proposes an integrated Bayesian framework for feature-based simultaneous localisation and map building (SLAM) in the general case of uncertain feature number and data association. By modeling the measurements and feature map as random finite sets (RFSs), a formulation of the feature-based SLAM problem is presented that jointly estimates the number and location of the features, as well as the vehicle trajectory. More concisely, the joint posterior distribution of the set-valued map and vehicle trajectory is propagated forward in time as measurements arrive, incorporating both data association and feature management into a single recursion. Furthermore, the Bayes optimality of the proposed approach is established.**

A first order solution, coined the probability hypothesis density (PHD) SLAM filter, is derived, which jointly propagates the posterior PHD of the map and the posterior distribution of the vehicle trajectory. A Rao-Blackwellised implementation of the PHD-SLAM filter is proposed based on the Gaussian mixture PHD filter (for the map) and a particle filter (for the vehicle trajectory). Simulated and experimental results demonstrate the merits of the proposed approach, particularly in situations of high clutter and data association ambiguity.

***Index Terms*—Bayesian SLAM, Random Finite Set (RFS), Feature-based Map, Probability Hypothesis Density (PHD), Point Process.**

NOMENCLATURE

k	Current time index
M_k	Feature map random vector
$\hat{M}_k$	Estimate of M_k
X_k	Vehicle pose random vector at k
$X_{0:k}$	Vehicle trajectory random vector
$\hat{X}_{0:k}$	Estimate of $X_{0:k}$
$\mathcal{M}$	Feature map random finite set (RFS)
$\mathcal{M}_k$	Explored map RFS up to k
$\hat{\mathcal{M}}_k$	Estimate of $\mathcal{M}_k$
$\mathcal{Z}_k$	RFS sensor measurement
$\mathcal{Z}_{0:k}$	History of RFS measurements
$\mathcal{D}_k$	Feature measurement RFS
$\mathcal{C}_k$	Clutter measurement RFS
$\mathcal{B}_k$	RFS of the new features
$p_{k\|k}(\mathcal{M}_k,X_{0:k}\|\cdot)$	Conditional pdf of RFS-SLAM
$p_{k\|k}(\mathcal{M}_k\|\cdot)$	Conditional pdf of $\mathcal{M}_k$
$p_{k\|k-1}(\mathcal{M}_k\|\cdot)$	Predicted conditional pdf of $\mathcal{M}_k$
$g_k(\mathcal{Z}_k\|\cdot)$	Conditional pdf of $\mathcal{Z}_k$
$f_{\mathcal{M}}(\cdot\|\mathcal{M}_{k-1})$	Transition density of the map RFS
$f_X(\cdot\|X_{k-1})$	Vehicle transition density
$f_{\mathcal{D}}(\cdot)$	Density of the feature measurement RFS
$f_{\mathcal{C}}(\cdot)$	Density of the clutter measurement RFS
$f_{\mathcal{B}}(\cdot)$	Density of the new feature RFS
$v_{k\|k}(m\|\cdot)$	PHD of the explored map RFS, $\mathcal{M}_k$
$v_{k\|k-1}(m\|\cdot)$	PHD of the predicted map, $\mathcal{M}_{k\|k-1}$
$c_k(z\|\cdot)$	PHD of $\mathcal{C}_k$
$b_k(m\|\cdot)$	PHD of $\mathcal{B}_k$
$\mathfrak{m}_k$	Number of features in $\mathcal{M}_k$
$\hat{\mathfrak{m}}_k$	Estimated number of features in $\mathcal{M}_k$
m^i	i^{th} feature in $\mathcal{M}_k$
$\mathfrak{z}_k$	Number of measurements in $\mathcal{Z}_k$
z^i	i^{th} measurement in $\mathcal{Z}_k$
$g_k(z\|m)$	Likelihood of z given feature m
$P_D(m)$	Detection probability of feature m
N	Number of particles
$X_{0:k}^{(i)}$	i^{th} sample trajectory
$w_k^{(i)}$	Weight of i^{th} sample trajectory
$v_k^{(i)}(m\|X_{0:k}^{(i)})$	i^{th} trajectory conditioned PHD of $\mathcal{M}_k$
$J_k^{(i)}$	Number of Gaussian components in the i^{th} trajectory conditioned PHD of $\mathcal{M}_k$
$\eta_k^{(i,j)}$	Weight of the j^{th} Gaussian component of the i^{th} trajectory conditioned PHD of $\mathcal{M}_k$
$\mu_k^{(i,j)}$	Mean of the j^{th} Gaussian component of the i^{th} trajectory conditioned PHD of $\mathcal{M}_k$
$P_k^{(i,j)}$	Covariance of the j^{th} Gaussian component of the i^{th} trajectory conditioned PHD of $\mathcal{M}_k$
$\bar{d}^{(c)}(\hat{\mathcal{M}}_k,\mathcal{M}_k)$	Error between $\hat{\mathcal{M}}_k$ and $\mathcal{M}_k$, with cut-off parameter c

I. INTRODUCTION

FOLLOWING seminal developments in autonomous robotics [1], the problem of simultaneous localisation and mapping (SLAM) gained widespread interest, with numerous potential applications ranging from robotic planetary exploration to intelligent surveillance. This paper focusses on the feature-based approach that decomposes physical environmental landmarks into parametric representations such as points, lines, circles, corners, etc., known as features. Feature-based maps are comprised of an unknown number of features at unknown spatial locations [2], and are widely used in the SLAM literature [3], [4], [5], [6], [7]. Estimating a feature map, thus requires the joint estimation of the *number* and location of the features which have been covered by the sensor's field-of-view (FoV).

In the Bayesian paradigm, the feature-based SLAM problem (henceforth referred to as SLAM for compactness) amounts to jointly propagating the posterior distribution of the map and vehicle trajectory. Current state-of-the-art SLAM solutions comprise two separate steps [6]:

- determine the measurement (to feature) associations; and

This work was presented in part at the IEEE International Conference on Robotics and Automation, Anchorage, Alaska, USA, May 3 - 8, 2010.

John Mullane is with the school of Electrical & Electronic Engineering, Nanyang Technological University, Singapore. Martin Adams is with the Department of Electrical Engineering, University of Chile, Santiago, Chile. Ba-Ngu Vo and Ba-Tuong Vo are with the School of Electrical, Electronic and Computer Engineering, University of Western Australia. (email: jsmullane@ntu.edu.sg)

- given the associations, estimate the feature locations and vehicle pose via stochastic filtering.

This two-tiered approach is efficient and works well for a wide range of applications [4], [6], [7] but is sensitive to data association (DA) uncertainty [8]. A SLAM solution that is robust to DA uncertainty under high clutter and measurement noise requires a framework that fully integrates DA uncertainty into the estimation of the map (and vehicle trajectory).

This paper advocates a fully integrated Bayesian framework for SLAM under DA uncertainty and unknown feature number. The key to this formulation is the representation of the map as a *finite set* of features. Indeed, from an estimation viewpoint, it is argued in section II-A that the map should be represented by a finite set. Using Random Finite Set (RFS) theory, SLAM is then posed as a Bayesian filtering problem in which the joint posterior distribution of the vehicle trajectory and set-valued map are propagated forward in time as measurements arrive. This so-called RFS-SLAM framework allows for the joint recursive estimation of the vehicle trajectory, the feature locations and the number of features in the map. Moreover, it is shown that the proposed RFS approach is Bayes optimal.

The RFS formulation for SLAM was first proposed in [9] with preliminary studies using 'brute force' implementations also appearing in [10]. The approach modeled the joint vehicle trajectory and map as a single RFS, and recursively propagates its first order moment. In this paper, however, a tractable first order approximation, coined the (Probability Hypothesis Density) PHD-SLAM filter, is derived, which first factorises the RFS-SLAM density, then propagates the posterior PHDs of multiple trajectory-conditioned maps and the posterior distribution of the vehicle trajectory. The PHD is the first order moment of the RFS of the map and is closely related to the occupancy grid representation, as discussed later in section IV-B. Furthermore, as presented in this paper, the RFS approach to SLAM admits the concept of an 'expected' map via the PHD construct, which is not available in existing SLAM approaches.

This factorised approach to SLAM was established in the, now well known, FastSLAM concept [6]. However, it will be shown that the same factorisation method applied to vectors in FastSLAM, cannot be applied to sets, since it results in invalid densities in the feature space. Therefore one of the main contributions of this paper is a technique which allows such a factorisation to be applied to sets in a principled manner. Preliminary results have been announced in [11] and this paper presents a more rigorous analysis of the RFS approach to SLAM, an improved version of the PHD-SLAM filter, a discussion of Bayes optimality, as well as simulated and real experimental results. The merits of the RFS approach are demonstrated, particularly in situations of high clutter and data association ambiguity.

The paper is organised as follows: Section II demonstrates that the feature map can be represented as a finite-set of features and proposes a corresponding Bayesian filtering framework for SLAM. Given the joint posterior density of the random vector vehicle trajectory and RFS feature map, optimal estimators are introduced and discussed in section III. The PHD-SLAM filter, which propagates the first-order-moment of the RFS map, is presented in section IV. Section V outlines a Rao-Blackwellised implementation of the PHD-SLAM filter, with section VI presenting and discussing its performance. Extensions of the approach to incorporate other useful RFS representations are also presented.

II. Bayesian RFS (Feature-based) SLAM

This section discusses the mathematical representation of the map and presents a Bayesian formulation of the SLAM problem subject to uncertainty in DA and the number of features. In particular, it is argued that fundamentally, the map should be represented as a finite set and thus the concept of a random finite set is required for a Bayesian SLAM formulation.

A. Mathematical representation of the Feature Map

This subsection demonstrates that, in the context of jointly estimating the number of features and their locations, the collection of features, referred to as the feature map, is naturally represented by a finite set. The rationale behind this representation traces back to a fundamental consideration in estimation theory - estimation error. Without a meaningful notion of estimation error, estimation has very little meaning. Despite the fact that mapping error is equally as important as localisation error, its formal treatment has been largely neglected. To illustrate this point, recall that in existing SLAM formulations the map is constructed by stacking features into a vector, and consider the simplistic scenarios depicted in Figure 1.

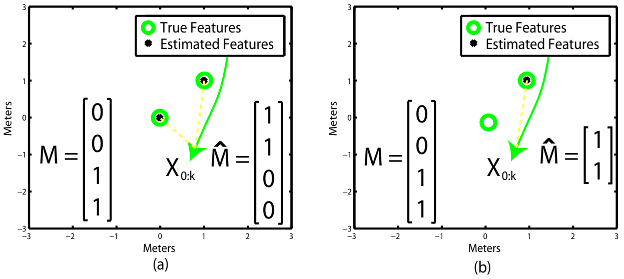

Fig. 1. A hypothetical scenario showing a fundamental inconsistency with vector representations of feature maps. If M is the true map, how should the error be assigned when the number of features in the map estimate, $\hat{M}$, is incorrect?

Figure 1a depicts a scenario in which there are two true features at coordinates $(0, 0)$ and $(1, 1)$. The true map, M, is then represented by the vector $M = [0\ 0\ 1\ 1]^T$. If features are stacked into a vector in order of appearance then, given a vehicle trajectory $X_{0:k}$ (e.g. as shown in the figure) and perfect measurements, the estimated map may be given by the vector $\hat{M} = [1\ 1\ 0\ 0]^T$. Despite a seemingly perfect estimate of the map, the Euclidean error of the estimated map, $||M - \hat{M}||$, is 2. This inconsistency arises because the ordering of the features in the representation of the map should not be relevant. A vector representation however, imposes a mathematically strict arrangement of features in the estimated map based on the order in which they were detected [1], [5]. Intuitively, the elements of $\hat{M}$ could be permuted to obtain a zero error, however, the representation of all possible permutations of the elements of a vector is, by definition, a set. Hence, such a permuting operation implies that the resulting error distance is no longer a distance for vectors but a distance for sets, and thus this paper derives a set based approach to SLAM. Another problem is depicted in Figure 1b, in which there are again two features at (0,0) and (1,1), but due to a missed detection (for instance), the estimated map comprises only one feature at (1,1). In such a situation, it is difficult to define a mathematically consistent error metric (Euclidean error, Mean Squared Error) between the vectors M and $\hat{M}$ since they contain a different number of elements. It is evident from these examples that stacking individual features into a single vector does not lead to a natural notion of mapping error, in general.

A *finite set* representation of the map, $\mathcal{M}_k = \{m_k^1, \ldots, m_k^{\mathfrak{m}_k}\}$, where $m_k^1, \ldots, m_k^{\mathfrak{m}_k}$ are the $\mathfrak{m}_k$ features present at time k, admits a natural notion of estimation error since the ‘distance’, or error between sets, is a well understood concept, for example, the Hausdorff, OMAT [12] and OSPA [13] distances.

It should be noted that, while finite-sets naturally capture the intrinsic properties of a feature map, a finite set map representation for grid-based frameworks [14], is unnecessary since the number of grid cells is known (*a priori* tessellation), and the order of the map states signifies their spatial location in the grid. As such, grid map estimation errors can be readily defined via Euclidean, Mean Squared or Sum of Squared Error metrics [15]. Due to the fundamentally different estimation state-space of grid maps, being in occupancy space, it is difficult to draw comparison between grid-based SLAM algorithms and the RFS feature-based framework proposed in this paper.

For most sensor models considered in SLAM, the order in which sensor readings are recorded at each sampling instance simply depends on the direction in which the vehicle/sensor points and has no significance on the state of the map, which typically evolves in a globally defined coordinate system, independent of the vehicle's pose. Moreover, the number of measurements, $\mathfrak{z}_k$, at any given time is not fixed due to detection uncertainty, spurious measurements and unknown number of features. Thus, this type of measurement may also be naturally represented by a *finite set* of readings, $\mathcal{Z}_k = \{z_k^1, z_k^2, \ldots, z_k^{\mathfrak{z}_k}\}$.

B. RFS-SLAM

This section outlines the RFS-SLAM model followed by the Bayesian RFS-SLAM Filter.

1) The RFS-SLAM Model: In the Bayesian estimation paradigm, the states/parameters and measurements are treated as realizations of random variables. Since the map (and the measurement) is more appropriately represented by a finite set, in such a framework, the concept of a random finite set is required for Bayesian map estimation, [9]. Similar to a random vector being a vector-valued random variable (vehicle trajectory for instance), a *random finite set* (RFS) is simply a finite-set-valued random variable. Moreover, similar to random vectors, the probability density (if it exists) is a very useful descriptor of an RFS, especially in filtering and estimation. However, the space of finite sets does not inherit the usual Euclidean notion of integration and density. Hence, standard tools for random vectors are not appropriate for random finite sets. Mahler's Finite Set Statistics (FISST) provide practical mathematical tools for dealing with RFSs [16], [17], based on a notion of integration and density that is consistent with point process theory [18]. This approach has attracted substantial research interest in the multi-target tracking community [19], with a more comprehensive list of applications appearing in [17]. An informal introduction to RFS estimation can be found in [20], with a detailed description of the latest advances available in [21], [22].

Let $\mathcal{M}$ be the RFS representing the entire unknown and unexplored static map and let $\mathcal{M}_{k-1}$ be the RFS representing the subset of that map which has been explored, i.e. that has passed through the field-of-view (FoV) of the vehicle mounted sensor i.e.

$$\mathcal{M}_{k-1} = \mathcal{M} \cap FoV(X_{0:k-1}). \tag{1}$$

Note that $FoV(X_{0:k-1}) = FoV(X_0) \cup FoV(X_1) \cup \cdots \cup FoV(X_{k-1})$. $\mathcal{M}_{k-1}$ therefore represents the set on the space of features which intersects with the union of individual FoVs, over the vehicle trajectory up to and including time $k-1$. Given this representation, the explored map $\mathcal{M}_{k-1}$ evolves in time according to,

$$\mathcal{M}_k = \mathcal{M}_{k-1} \cup \Big(FoV(X_k) \cap \bar{\mathcal{M}}_{k-1} \Big) \tag{2}$$

where $\bar{\mathcal{M}}_{k-1} = \mathcal{M} - \mathcal{M}_{k-1}$ (note the difference operator used here is the set difference), i.e the set of features that are not in $\mathcal{M}_{k-1}$. Let the new features which have entered the FoV, i.e. the second term of (2), be modeled by the independent RFS, $\mathcal{B}_k(X_k)$. In this case, the RFS map transition density is given by,

$$f_{\mathcal{M}}(\mathcal{M}_k|\mathcal{M}_{k-1}, X_k) = \sum_{\mathcal{W} \subseteq \mathcal{M}_k} f_{\mathcal{M}}(\mathcal{W}|\mathcal{M}_{k-1}) f_{\mathcal{B}}(\mathcal{M}_k - \mathcal{W}|X_k) \tag{3}$$

where $f_{\mathcal{M}}(\mathcal{W}|\mathcal{M}_{k-1})$ is the transition density of the set of features that are in the $FoV(X_{0:k-1})$ at time $k-1$ to time k, and $f_{\mathcal{B}}(\mathcal{M}_k - \mathcal{W}|X_k)$ is the density of the RFS, $\mathcal{B}(X_k)$, of the new features that pass within the field of view at time k. Modeling the vehicle dynamics by the standard Markov process with transition density $f_X(X_k|X_{k-1}, U_k)$, where U_k denotes the control input at time k, the joint transition density of the map and the vehicle pose can be written as,

$$f_{k|k-1}(\mathcal{M}_k, X_k|\mathcal{M}_{k-1}, X_{k-1}, U_k) = f_{\mathcal{M}}(\mathcal{M}_k|\mathcal{M}_{k-1}, X_k) f_X(X_k|X_{k-1}, U_k). \tag{4}$$

The measurement $\mathcal{Z}_k$ received by the vehicle with pose X_k, at time k, can be modeled by

$$\mathcal{Z}_k = \bigcup_{m \in \mathcal{M}_k} \mathcal{D}_k(m, X_k) \cup \mathcal{C}_k(X_k) \tag{5}$$

where $\mathcal{D}_k(m, X_k)$ is the RFS of measurements generated by a feature at m and $\mathcal{C}_k(X_k)$ is the RFS of the spurious measurements at time k, which may depend on the vehicle pose X_k. Therefore $\mathcal{Z}_k$ consists of a random number, $\mathfrak{z}_k$, of measurements, whose order of appearance has no physical significance with respect to the estimated map of features. It is also assumed that all $\mathcal{D}_k(m, X_k)$, and $\mathcal{C}_k(X_k)$ are independent RFSs when conditioned on X_k.

The RFS of the measurements generated by a feature at m can be modeled by a Bernoulli RFS[1] [17] given by, $\mathcal{D}_k(m, X_k) = \emptyset$ with probability $1 - p_D(m|X_k)$ and $\mathcal{D}_k(m, X_k) = \{z\}$ with probability density $p_D(m|X_k)g_k(z|m, X_k)$. For a given robot pose X_k, $p_D(m|X_k)$ is the probability of the sensor detecting a feature at m. Given a detection, $g_k(z|m, X_k)$ is then the likelihood that a feature at m generates the measurement z. The assumed Poisson RFS $\mathcal{C}_k(X_k)$ represents the spurious measurements, which may be dependent on the vehicle pose, X_k.

Using Finite Set Statistics [17], the likelihood of the measurement $\mathcal{Z}_k$ is then given by,

$$g_k(\mathcal{Z}_k|X_k, \mathcal{M}_k) = \sum_{\mathcal{W} \subseteq \mathcal{Z}_k} f_{\mathcal{D}}(\mathcal{W}|\mathcal{M}_k, X_k) f_{\mathcal{C}}(\mathcal{Z}_k - \mathcal{W}|X_k) \quad (6)$$

with $f_{\mathcal{D}}(\mathcal{W}|\mathcal{M}_k, X_k)$ denoting the density of the RFS of observations, and $f_{\mathcal{C}}(\mathcal{Z}_k - \mathcal{W}|X_k)$ denoting the density of the clutter RFS, $\mathcal{C}_k(X_k)$. It can be seen that this likelihood directly encapsulates the inherent measurement uncertainty, with $f_{\mathcal{D}}(\mathcal{W}|\mathcal{M}_k, X_k)$ considering detection uncertainty and measurement noises, and $f_{\mathcal{C}}(\mathcal{Z}_k - \mathcal{W}|X_k)$ modeling the spurious measurements. This density is typically *a priori* given as Poisson in number and uniform in space [3]. The Bayesian RFS-SLAM filter is next outlined.

2) The RFS-SLAM Filter: Let the joint posterior density of the map $\mathcal{M}_k$ be denoted by $p_k(\mathcal{M}_k, X_{1:k}|Z_{1:k}, U_{1:k}, X_0)$ and the vehicle trajectory by $X_{0:k}$. For clarity of exposition, the following abbreviations shall be adhered to,

$$p_{k|k-1}(\mathcal{M}_k, X_{1:k}) = p_{k|k-1}(\mathcal{M}_k, X_{1:k}|Z_{0:k}, U_{0:k-1}, X_0)$$
$$p_k(\mathcal{M}_k, X_{1:k}) = p_k(\mathcal{M}_k, X_{1:k}|Z_{0:k}, U_{0:k-1}, X_0)$$

The recursion for a static feature map is then given as follows,

$$p_{k|k-1}(\mathcal{M}_k, X_{1:k}) = f_X(X_k|X_{k-1}, U_k) \times \int f_{\mathcal{M}}(\mathcal{M}_k|\mathcal{M}_{k-1}, X_k) p_{k-1}(\mathcal{M}_{k-1}, X_{1:k-1}) \delta\mathcal{M}_{k-1} \quad (7)$$

$$p_k(\mathcal{M}_k, X_{1:k}) = \frac{g_k(\mathcal{Z}_k|X_k, \mathcal{M}_k) p_{k|k-1}(\mathcal{M}_k, X_{1:k})}{g_k(\mathcal{Z}_k|\mathcal{Z}_{0:k-1}, X_0)} \quad (8)$$

where the δ denotes a set integral[2].

The joint posterior density encapsulates all statistical information about the map and vehicle pose, that can be inferred from the measurements and control history up to time k. The RFS-SLAM recursion (8) integrates uncertainty in DA and number of features into a single Bayesian filter and does not require a separate DA step or any form of feature management, as is classically required [5], [6], [8].

The outputs of a SLAM algorithm are the estimate of the vehicle trajectory and the map. In a Bayesian approach, these are computed from the joint posterior density in (8). The following section establishes Bayes optimality for various RFS-SLAM estimators, while section IV presents a tractable solution of the RFS-SLAM recursion.

III. Bayes Optimal RFS-SLAM Estimators

This section discusses various Bayes estimators for the SLAM problem and their optimality, based on a vector representation of the vehicles trajectory, and a finite-set representation of the map. The notion of Bayes optimal estimators is fundamental to the Bayesian estimation paradigm. In general, if the function $\hat{\theta} : z \mapsto \hat{\theta}(z)$ is an estimator of a parameter θ, based on a measurement z, and $C(\hat{\theta}(z), \theta)$ is the cost for using $\hat{\theta}(z)$ to estimate θ, then the Bayes risk $R(\hat{\theta})$ is the expected cost over all possible realisations of the measurement and parameter, i.e

$$R(\hat{\theta}) = \int\int C(\hat{\theta}(z), \theta) p(z, \theta) d\theta dz \quad (9)$$

where $p(z, \theta)$ is the joint probability density of the measurement z and the parameter θ. A Bayes optimal estimator is any estimator that minimises the Bayes risk [23], [24].

In the SLAM context, relevant Bayes optimal estimators are those for the vehicle trajectory and the map. The posterior densities $p_k(X_{1:k}) \triangleq p_k(X_{1:k}|Z_{0:k}, U_{0:k-1}, X_0)$ and $p_k(\mathcal{M}_k) \triangleq p_k(\mathcal{M}_k|Z_{0:k}, U_{0:k-1}, X_0)$ for the vehicle trajectory and map, can be obtained by marginalising the joint posterior density, $p_k(\mathcal{M}_k, X_{1:k}|Z_{0:k}, U_{0:k-1}, X_0)$. For the vehicle trajectory, the posterior mean, which minimises the mean squared error (MSE), is a widely used Bayes optimal estimator. However, since the map is more appropriately represented as a finite set, the notion of MSE does not apply. Moreover, standard Bayes optimal estimators are defined for vectors and subsequently do not apply to finite-set feature maps. To the best of the authors' knowledge, there is no work which establishes Bayes optimality of estimators for finite-set feature maps (and consequently feature-based SLAM in terms of taking the estimated number of features into account).

A. Optimal Feature Map Estimation

In the following, as before, let $\mathcal{M}_k$ denote the feature-based map state at time k comprising $\mathfrak{m}_k$ features and $p_k(\mathcal{M}_k)$ denote its posterior spatial density. If $\hat{\mathcal{M}}_k : Z_{1:k} \mapsto \hat{\mathcal{M}}_k(Z_{1:k})$ is an estimator of the feature map $\mathcal{M}_k$, and $C(\hat{\mathcal{M}}_k(Z_{1:k}), \mathcal{M}_k)$ is the cost for using $\hat{\mathcal{M}}_k(Z_{1:k})$ to estimate $\mathcal{M}_k$, then the Bayes risk for mapping is given by

$$R(\hat{\mathcal{M}}_k) = \int\int C(\hat{\mathcal{M}}_k(Z_{1:k}), \mathcal{M}_k) p_k(\mathcal{M}_k, Z_{1:k}) \delta\mathcal{M}_k \delta\mathcal{Z}_{1:k}. \quad (10)$$

[1] The Bernoulli RFS is empty with a probability $1 - \epsilon$ and is distributed according to a density π with probability ϵ.

[2] Since the integration variable (the map) is a finite set, the usual definition of integration for vectors does not apply. In this case a set integral is required. For more details see [17], [18].

where $p_k(\mathcal{M}_k, Z_{1:k})$ is the joint density of the map and measurement history. Since, due to the arguments presented in section II-A, the map and measurements are more appropriately represented as sets, the Bayes risk above is defined in terms of set integrals[2]. Several principled solutions to performing feature map estimation such as the Joint Multi-object Estimator or Marginal Multi-object Estimator [17] can be applied, as can the PHD Estimator, which is next described and adopted in this paper.

B. The PHD Estimator

An intuitive approach to RFS state estimation is to exploit the physical interpretation of the first moment of an RFS, its PHD, v_k [17]. For a map RFS $\mathcal{M}_k$, the PHD is a non-negative function v, such that for each region S in the space of features,

$$\int_S v_k(m)dm = \mathbb{E}[|\mathcal{M}_k \cap S|]. \tag{11}$$

The mass of the PHD gives the expected number of features, $\hat{\mathfrak{m}}_k$, in the map $\mathcal{M}_k$ and its peaks indicate locations with high probability of feature existence. A discussion on the optimality/suboptimality of the PHD estimator is provided in [22].

If the RFS $\mathcal{M}_k$ is Poisson, i.e. the number of points is Poisson distributed and the points themselves are independently and identically distributed (iid), then the probability density of $\mathcal{M}_k$ can be constructed exactly from the PHD,

$$p(\mathcal{M}_k) = \frac{\prod\limits_{m \in \mathcal{M}_k} v_k(m)}{\exp(\int v_k(m)dm)}. \tag{12}$$

In this sense, the PHD can be thought of as a 1st moment approximation of the probability density of an RFS.

IV. The PHD-SLAM Filter

Since the full RFS-SLAM filter is numerically intractable, it is necessary to look for tractable but principled approximations. The probability hypothesis density (PHD) approach which propagates the 1st order moment of the posterior multi-target RFS has proven to be both powerful and effective in multi-target filtering [17]. However, this technique cannot be directly applied to SLAM which propagates the joint posterior density of the map and the vehicle trajectory.

This section derives a recursion that jointly propagates the posterior PHD of the map and the posterior density of the vehicle trajectory. Analogous to FastSLAM, the RFS-SLAM recursion can be factorised as shown in subsection IV-A. Subsection IV-B discusses the PHD estimator in the context of this factorised recursion. Subsection IV-D presents a trajectory-conditioned mapping algorithm based on the PHD, while subsection IV-E extends this mapping algorithm to perform SLAM.

A. The Factorised RFS-SLAM Recursion

Using standard conditional probability, the joint posterior RFS-SLAM density of (8) can be decomposed as,

$$\begin{aligned} p_k(\mathcal{M}_k, X_{1:k}|\mathcal{Z}_{0:k}, U_{0:k-1}, X_0) &= \\ p_k(X_{1:k}|\mathcal{Z}_{0:k}, U_{0:k-1}, X_0)&p_k(\mathcal{M}_k|\mathcal{Z}_{0:k}, X_{0:k}). \end{aligned} \tag{13}$$

Thus, the recursion for the joint RFS map-trajectory posterior density according to (8) is equivalent to jointly propagating the posterior density of the map conditioned on the trajectory and the posterior density of the trajectory. In this section, as before, for compactness,

$$\begin{aligned} p_{k|k-1}(\mathcal{M}_k|X_{0:k}) &= p_{k|k-1}(\mathcal{M}_k|\mathcal{Z}_{0:k-1}, X_{0:k}) \\ p_k(\mathcal{M}_k|X_{0:k}) &= p_k(\mathcal{M}_k|\mathcal{Z}_{0:k}, X_{0:k}) \\ p_k(X_{1:k}) &= p_k(X_{1:k}|\mathcal{Z}_{0:k}, U_{0:k-1}, X_0) \end{aligned}$$

and it follows that,

$$\begin{aligned} p_{k|k-1}(\mathcal{M}_k|X_{0:k}) = \int f_{\mathcal{M}}(\mathcal{M}_k|\mathcal{M}_{k-1}, X_k)\times \\ p_{k-1}(\mathcal{M}_{k-1}|X_{0:k-1})\delta\mathcal{M}_{k-1} \end{aligned} \tag{14}$$

$$p_k(\mathcal{M}_k|X_{0:k}) = \frac{g_k(\mathcal{Z}_k|\mathcal{M}_k, X_k)p_{k|k-1}(\mathcal{M}_k|X_{0:k})}{g_k(\mathcal{Z}_k|\mathcal{Z}_{0:k-1}, X_{0:k})} \tag{15}$$

$$\begin{aligned} p_k(X_{1:k}) = g_k(\mathcal{Z}_k|\mathcal{Z}_{0:k-1}, X_{0:k})\times \\ \frac{f_X(X_k|X_{k-1}, U_{k-1})p_{k-1}(X_{1:k-1})}{g_k(\mathcal{Z}_k|\mathcal{Z}_{0:k-1})}. \end{aligned} \tag{16}$$

Apart from adopting RFS likelihoods for the measurement and map, the recursion defined by (14), (15), (16) is similar to that in FastSLAM [6], [25]. However, the use of RFS likelihoods has important consequences in the evaluation of (16), to be seen later in section IV-E. In FastSLAM, it should be noted that the map recursion of (15) is further decomposed into the product of K independent densities for each of the K features assumed to exist in the map. Furthermore, FastSLAM is conditioned on the inherently unknown data association assignments. In contrast, RFS-SLAM is not conditioned on any data association hypotheses to determine the number of features to estimate and the recursion of (15) is that of a RFS feature map. Consequently, the propagation of the map involves probability densities of random finite sets and marginalisation over the map involves set integrals. Similar to FastSLAM, the effect of the trajectory conditioning on RFS-SLAM is to render each feature estimate conditionally independent and thus the map correlations, critical to EKF-SLAM [5], are not required.

B. The PHD in RFS-SLAM

Recall from section III-A, that an optimal estimator for a random vector is the conditional expectation. Many state-of-the-art SLAM algorithms adopt Sequential Monte Carlo (SMC) methods. It is well known that SMC techniques are more amenable to expectation operations than maximisation operations, since if p is approximated by a set of weighted samples $\{w^{(i)}, X^{(i)}\}_{i=1}^{N}$, then [26], [27],

$$\sum_{i=1}^{N} w^{(i)} X^{(i)} \rightarrow \mathbb{E}[X] \tag{17}$$

as $N \rightarrow \infty$. However, in FastSLAM [6], it is common to choose the trajectory sample with the highest weight as the estimate of the vehicle path, and its corresponding map, as the estimate of the map. It is easier to establish convergence in SMC implementations if we use the expected path and expected map. However, it is not clear how the expected map is interpreted.

The PHD construct allows an alternative notion of expectation for maps, thereby fully exploiting the advantage of an SMC approximation. The PHD, v, is a function defined on the feature space satisfying (11). The value of the PHD at a point gives the expected number of features at that point while the integral over any given region gives the expected number of features in that region. A salient property of the PHD construct in map estimation is that the posterior PHD of the map is indeed the expectation of the trajectory-conditioned PHDs. More concisely,

$$v_k(m) = \mathbb{E}\left[v_k(m|X_{1:k})\right], \tag{18}$$

where the expectation is taken over the vehicle trajectory $X_{1:k}$. This result follows from standard properties of the PHD (intensity function) of an RFS, see for example classical texts such as [28], [29]. Thus the PHD construct provides a natural framework to average feature map estimates, while incorporating both unknown associations and different feature numbers. This differs dramatically from vector based map averaging methods which require feature identification tracking and rule-based combinations [30]. In contrast, map averaging for grid-based maps is straight forward due to both known grid alignments and number of cells. While the practical merits of an expected feature map estimate for SLAM using a single sensor may be unclear at this time, related operations such as 'feature map addition' may be of use in sensor fusion and multi-robot SLAM applications. Furthermore, the PHD construct admits a Bayes optimal estimator for the map, as discussed previously in section III-A.

C. Evidence Grids and the PHD

As mentioned in the introduction, the PHD of a map is closely related to the occupancy grid representation. Intuitively, the PHD can be interpreted as a limiting case of the occupancy probability. Following [31], consider a grid system and let m_i, $B(m_i)$, denote the center and region defined by the boundaries of the ith grid cell. Let $P^{(occ)}(B(m_i))$ and $\lambda(B(m_i))$ denote the occupancy probability and the area of the ith grid cell. Assume that the grid is sufficiently fine so that each grid cell contains at most one feature, then the expected number of features over the region $S_J = \bigcup_{i\in J} B(m_i)$ is given by,

$$\begin{aligned}\mathbb{E}\left[|M \cap S_J|\right] &= \sum_{i\in J} P^{(occ)}(B(m_i)) \\ &= \sum_{i\in J} v(m_i)\lambda(B(m_i)).\end{aligned}$$

where $v(m_i) = \frac{P^{(occ)}(B(m_i))}{\lambda(B(m_i))}$. Intuitively, as the grid cell area tends to zero (or for an infinitesimally small cell) any region S can be approximated by $\bigcup_{i\in J} B(m_i)$, for some J. The sum then becomes an integral and the expected number of features in S becomes,

$$\mathbb{E}\left[|M \cap S|\right] = \int_S v(m)dm. \tag{19}$$

Hence the PHD $v(m)$ can be interpreted as the occupancy probability density at the point m. The recursive propagation of the PHD is discussed in the following section.

D. PHD Mapping

This subsection details the trajectory-conditioned PHD mapping recursion of (15), as was first proposed in [10]. The predicted and posterior RFS maps are approximated by Poisson RFSs with PHDs $v_{k|k-1}(m|X_{0:k})$ and $v_k(m|X_{0:k})$ respectively,

$$p_{k|k-1}(\mathcal{M}_k|X_{0:k}) \approx \frac{\prod_{m\in\mathcal{M}_k} v_{k|k-1}(m|X_{0:k})}{\exp\left(\int v_{k|k-1}(m|X_{0:k})dm\right)} \tag{20}$$

$$p_k(\mathcal{M}_k|X_{0:k}) \approx \frac{\prod_{m\in\mathcal{M}_k} v_k(m|X_{0:k})}{\exp\left(\int v_k(m|X_{0:k})dm\right)}. \tag{21}$$

In essence, this approximation assumes that features are iid and the number of features is Poisson distributed. This PHD approximation has been proven to be powerful and effective in multi-target tracking [17]. Poisson approximations for the number of new features have also been adopted in certain SLAM solutions [3].

Under these approximations, it has been shown [16] that, similar to standard recursive estimators, the PHD recursion has a *predictor-corrector* form. The PHD predictor equation is,

$$v_{k|k-1}(m|X_{0:k}) = v_{k-1}(m|X_{0:k-1}) + b(m|X_k) \tag{22}$$

where $b(m|X_k)$ is the PHD of the new feature RFS, $\mathcal{B}(X_k)$, discussed previously in section II-B. The PHD corrector equation is then,

$$\begin{aligned}v_k(m|X_{0:k}) = v_{k|k-1}(m|X_{0:k})\Bigg[1 - P_D(m|X_k) + \\ \sum_{z\in\mathcal{Z}_k} \frac{\Lambda(m|X_k)}{c_k(z|X_k) + \int \Lambda(\zeta|X_k)v_{k|k-1}(\zeta|X_{0:k})d\zeta}\Bigg]\end{aligned} \tag{23}$$

where $\Lambda(m|X_k) = P_D(m|X_k)g_k(z|m, X_k)$ and,

$P_D(m|X_k)$ = the probability of detecting a feature at m, from vehicle pose X_k.
$c_k(z|X_k)$ = PHD of the clutter RFS $\mathcal{C}_k$ in (5) at time k

The predictor of (22) comprises the sum of the previous PHD and the PHD of the set of static features hypothesised to enter the sensor's FoV due to vehicle motion. The corrector of (23) is governed by the following sensor characteristics [17]:

1) $P_D(m|X_k)$. If a feature at m is not in $FoV(X_k)$, it could not have been observed, thus $P_D(m|X_k) = 0$. From (23),

$$v_k(m|X_{0:k}) = v_{k|k-1}(m|X_{0:k})[1 - 0 + 0]$$

i.e. the updated PHD equals the predicted PHD, as no new information is available. On the other hand, if m is in $FoV(X_k)$ and $P_D(m|X_k) \approx 1$, the summation over all measurements tends to dominate. Then the predicted PHD is modified by the sum of terms dependent on the measurement likelihood and clutter PHD.

2) $c_k(z|X_k)$. A particular measurement could have originated from a feature or a false alarm. Assuming $P_D(m|X_k)$ is constant, and the number of false alarms is large and uniformly distributed in the region $FoV(X_k)$, the summation term of (23) is then dominated by $c_k(z|X_k)$. Since the measurement is likely to be a false alarm, it contributes little to the total posterior feature count, as it should. On the other hand, if the number of false alarms is low, $c_k(z|X_k)$ dominates less and the measurement contributes more to the value of the posterior PHD.

3) $g_k(z|m, X_k)$. Assume that the sensor model is accurate, thus $g_k(z|m, X_k)$ is large for the m which produces z. If z is consistent with prior information (the observation model), the numerator will dominate the summation of (23). Conversely if $g_k(z|m, X_k)$ is small and the measurement is unlikely to be from m, its corresponding term in the summation will have little influence.

A graphical depiction of a the posterior PHD after two consecutive measurements, approximated by a Gaussian Mixture, is shown respectively in Figures 2 and 3.

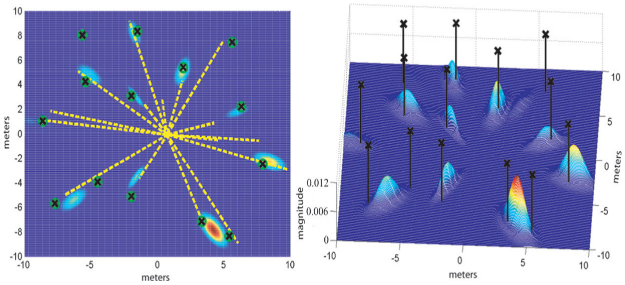

Fig. 2. A sample map PHD at time $k-1$, with the true map represented by black crosses. The measurement at $k-1$ is represented by the yellow dashed lines. The peaks of the PHD represent locations with highest concentration of expected number of features. The local PHD mass in the region of most features is 1, indicating the presence of 1 feature. The local mass close to some unresolved features (for instance at (5,-8)) is closer to 2, demonstrating the unique ability of the PHD function to jointly capture the number of features.

The PHD recursion is far more numerically tractable than propagating the RFS map densities of (15). In addition, the recursion can be readily extended to incorporate multiple sensors/vehicles by sequentially updating the map PHD with the measurement from each robot.

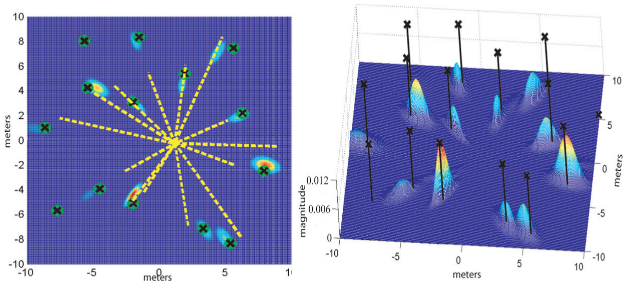

Fig. 3. The map PHD from figure 2 and the measurement at time k. Note that the features at (5,-8) are resolved due to well separated measurements, while at (-1,-4), a lone false alarm close to the feature measurement contributes to the local PHD mass. At (-5,-4) a small likelihood over all measurements, coupled with a moderate $c_k(z|X_k)$ results in a reduced local mass.

E. PHD-SLAM

This subsection extends the trajectory-conditioned PHD mapping recursion to the SLAM problem. With the hindsight of FastSLAM [6], the most obvious extension of PHD mapping [10] to SLAM is to exploit the factorisation (14), (15), (16), e.g. PHD for mapping and particle filtering for localisation. This technique requires the computation of the posterior density of the vehicle trajectory in (16), in particular the term $g_k(\mathcal{Z}_k|\mathcal{Z}_{0:k-1}, X_{0:k})$, which requires set integration,

$$g_k(\mathcal{Z}_k|\mathcal{Z}_{0:k-1}, X_{0:k}) = \int p(\mathcal{Z}_k, \mathcal{M}_k|\mathcal{Z}_{0:k-1}, X_{0:k})\delta\mathcal{M}_k. \tag{24}$$

This set integral is numerically intractable and a naive approach is to directly apply the EKF approximation proposed for FastSLAM [32]. However, an EKF approximation cannot be used since the likelihood (24), defined on the space of finite-sets, and its Fast-SLAM counterpart, defined on a Euclidean space, are two fundamentally different quantities and it is not known how they are even related. Therefore, in this case, it is fundamentally incorrect to use the EKF approximation in [6] as it will not result in a valid density, and thus its product with (15) cannot give the joint posterior of the map and pose.

Fortunately, by rearranging (15), it can be seen that $g_k(\mathcal{Z}_k|\mathcal{Z}_{0:k-1}, X_{0:k})$ is merely the normalising constant,

$$g_k(\mathcal{Z}_k|\mathcal{Z}_{0:k-1}, X_{0:k}) = \frac{g_k(\mathcal{Z}_k|\mathcal{M}_k, X_k)p_{k|k-1}(\mathcal{M}_k|X_{0:k})}{p_k(\mathcal{M}_k|X_{0:k})}. \tag{25}$$

Note in the above, that the LHS does not contain the variable $\mathcal{M}_k$, while the RHS has $\mathcal{M}_k$ in both the denominator and numerator. In essence, $\mathcal{M}_k$ in (25) is a dummy variable, and thus (25) holds for any arbitrary choice of $\mathcal{M}_k$. This allows the substitution of any choice of $\mathcal{M}_k$ to evaluate $g_k(\mathcal{Z}_k|\mathcal{Z}_{0:k-1}, X_{0:k})$. This is an important result, which allows for the likelihood of the measurement conditioned on the trajectory (but not the map), to be calculated in closed-form, as opposed to using the EKF approximations in [6]. The following considers two simple choices:

1) The empty map: Setting $\mathcal{M}_k = \emptyset$, and using the Poisson RFS approximations, (20) and (21), as well as the RFS measurement likelihood, (6), it follows that (see Appendix A),

$$g_k(\mathcal{Z}_k|\mathcal{Z}_{0:k-1}, X_{0:k}) \approx \kappa_k^{\mathcal{Z}_k} \times \exp\left(\hat{\mathfrak{m}}_k - \hat{\mathfrak{m}}_{k|k-1} - \int c_k(z|X_k)dz\right), \quad (26)$$

where, $\kappa_k^{\mathcal{Z}_k} = \prod_{z \in \mathcal{Z}_k} c_k(z|X_k)$ with, $c_k(z|X_k)$ being the PHD of the measurement clutter RFS $\mathcal{C}_k(X_k)$. In addition, $\hat{\mathfrak{m}}_k = \int v_k(m|X_{0:k})dm$ and $\hat{\mathfrak{m}}_{k|k-1} = \int v_{k|k-1}(m|X_{0:k})dm$.

2) The single feature map: In a similar manner, to evaluate the normalising constant for the case of $\mathcal{M}_k = \{\bar{m}\}$, again using (20), (21), and (6),

$$g_k(\mathcal{Z}_k|\mathcal{Z}_{0:k-1}, X_{0:k}) \approx \frac{1}{\Gamma}\Bigg[\Bigg((1 - P_D(\bar{m}|X_k))\kappa_k^{\mathcal{Z}_k} + P_D(\bar{m}|X_k) \sum_{z \in \mathcal{Z}_k} \kappa_k^{\mathcal{Z}_k - \{z\}} g_k(z|\bar{m}, X_k)\Bigg) v_{k|k-1}(\bar{m}|X_{0:k})\Bigg] \quad (27)$$

with,

$$\Gamma = \exp\left(\hat{\mathfrak{m}}_k - \hat{\mathfrak{m}}_{k|k-1} - \int c_k(z)dz\right) v_k(\bar{m}|X_{0:k}). \quad (28)$$

For this choice of $\mathcal{M}_k$, $\bar{m}$ can be, for instance, the feature with the least uncertainty or the maximum measurement likelihood. It is possible to choose $\mathcal{M}_k$ with multiple features, however this will increase the computational burden. Due to the presence of the measurement likelihood term $g_k(z|\bar{m}, X_k)$, it is expected that, in general, the single feature map update will outperform that of the empty map update. Note that in (25), every choice of $\mathcal{M}_k$ would give the same result, however (26) and (27) use different *approximations* of $p_k(\mathcal{M}_k|X_{0:k})$, yielding slightly different results. The following section presents a Rao-Blackwellised implementation of the proposed PHD-SLAM filter.

V. Rao-Blackwellised Implementation of the PHD-SLAM Filter

Following the description of the PHD-SLAM filter in the previous section, a Rao-Blackwellised (RB) implementation is detailed in this section. In essence, a particle filter is used to propagate the vehicle trajectory in (16), and a Gaussian mixture (GM) PHD filter is used to propagate each trajectory-conditioned map PHD in (15). As such, let the PHD-SLAM density at time $k-1$ be represented by a set of N particles,

$$\left\{w_{k-1}^{(i)}, X_{0:k-1}^{(i)}, v_{k-1}^{(i)}(m|X_{0:k-1}^{(i)})\right\}_{i=1}^{N},$$

where $X_{0:k-1}^{(i)} = [X_0, X_1^{(i)}, X_2^{(i)}, \ldots, X_{k-1}^{(i)}]$ is the i^{th} hypothesised vehicle trajectory and $v_{k-1}^{(i)}(m|X_{0:k-1}^{(i)})$ is its map PHD. The filter then proceeds to approximate the posterior density by a new set of weighted particles,

$$\left\{w_k^{(i)}, X_{0:k}^{(i)}, v_k^{(i)}(m|X_{0:k}^{(i)})\right\}_{i=1}^{N},$$

as follows:

A. PHD Mapping

Let the prior map PHD for the i^{th} particle, $v_{k-1}^{(i)}(m|X_{k-1}^{(i)})$, be a Gaussian mixture of the form,

$$v_{k-1}(m|X_{k-1}^{(i)}) = \sum_{j=1}^{J_{k-1}^{(i)}} \eta_{k-1}^{(i,j)} \mathcal{N}\big(m; \mu_{k-1}^{(i,j)}, P_{k-1}^{(i,j)}\big) \quad (29)$$

which is a mixture of $J_{k-1}^{(i)}$ Gaussians, with $\eta_{k-1}^{(i,j)}$, $\mu_{k-1}^{(i,j)}$ and $P_{k-1}^{(i,j)}$ being the corresponding predicted weights, means and covariances respectively for the j^{th} Gaussian component of the map PHD of the i^{th} trajectory. Let the new feature intensity for the particle, $b(m|\mathcal{Z}_{k-1}, X_k^{(i)})$, from the sampled pose, $X_k^{(i)}$ at time k also be a Gaussian mixture of the form,

$$b(m|\mathcal{Z}_{k-1}, X_k^{(i)}) = \sum_{j=1}^{J_{b,k}^{(i)}} \eta_{b,k}^{(i,j)} \mathcal{N}\big(m; \mu_{b,k}^{(i,j)}, P_{b,k}^{(i,j)}\big) \quad (30)$$

where, $J_{b,k}^{(i)}$ defines the number of Gaussians in the new feature intensity at time k and $\eta_{b,k}^{(i,j)}$, $\mu_{b,k}^{(i,j)}$ and $P_{b,k}^{(i,j)}$ are the corresponding components. This is analogous to the proposal distribution in the particle filter and provides an initial estimate of the new features entering the map.

The predicted intensity is therefore also a Gaussian mixture,

$$v_{k|k-1}(m|X_k^{(i)}) = \sum_{j=1}^{J_{k|k-1}^{(i)}} \eta_{k|k-1}^{(i,j)} \mathcal{N}\big(m; \mu_{k|k-1}^{(i,j)}, P_{k|k-1}^{(i,j)}\big) \quad (31)$$

which consists of $J_{k|k-1}^{(i)} = J_{k-1}^{(i)} + J_{b,k}^{(i)}$ Gaussians representing the union of the prior map intensity, $v_{k-1}(m|X_{k-1}^{(i)})$, and the proposed new feature intensity, according to (22). Since the measurement likelihood is also of Gaussian form, it follows from (23) that the posterior map PHD, $v_k(m|X_k^{(i)})$ is then also a Gaussian mixture given by,

$$v_k(m|X_k^{(i)}) = v_{k|k-1}(m|X_k^{(i)})\Bigg[1 - P_D(m|X_k^{(i)}) + \sum_{z \in \mathcal{Z}_k} \sum_{j=1}^{J_{k|k-1}^{(i)}} v_{G,k}^{(i,j)}(z, m|X_k^{(i)})\Bigg]. \quad (32)$$

The components of the above equation are given by,

$$v_{G,k}^{(i,j)}(z, m|X_k^{(i)}) = \eta_k^{(i,j)}(z|X_k^{(i)}) \mathcal{N}(m; \mu_{k|k}^{(i,j)}, P_{k|k}^{(i,j)}) \quad (33)$$

$$\eta_k^{(i,j)}(z|X_k^{(i)}) = \frac{P_D(m|X_k^{(i)}) \eta_{k|k-1}^{(i,j)} q^{(i,j)}(z, X_k^{(i)})}{c(z) + \sum_{\ell=1}^{J_{k|k-1}^{(i)}} P_D(m|X_k^{(i)}) \eta_{k|k-1}^{(i,\ell)} q^{(i,\ell)}(z, X_k^{(i)})} \quad (34)$$

where, $q^{(i,j)}(z, X_k^{(i)}) = \mathcal{N}\big(z; H_k \mu_{k|k-1}^{(i,j)}, S_k^{(i,j)}\big)$. The terms $\mu_{k|k}$, $P_{k|k}$ and S_k can be obtained using any standard filtering technique such as EKF or UKF. In this paper, the EKF updates are adopted.

The clutter RFS, C_k, is assumed Poisson distributed [3] in number and uniformly spaced over the mapping region. Therefore the clutter intensity is given by, $c(z) = \lambda_c \mathcal{U}(z)$, where λ_c is the average number of clutter measurements and $\mathcal{U}(z)$ denotes a uniform distribution on the measurement space. As with other feature-based GM implementations [33], pruning and merging operations are required to curb the explosive growth in the number of Gaussian components of the posterior map PHD. These operations are carried out as in [34].

B. The Vehicle Trajectory

The proposed filter adopts a particle approximation of the posterior vehicle trajectory, $p_k(X_{1:k})$, which is sampled/re-sampled as follows:

Step 1: *Sampling Step*

- For $i = 1, ..., N$, sample $\widetilde{X}_k^{(i)} \sim f_X(\widetilde{X}_k^{(i)} | X_{k-1}^{(i)}, U_{k-1})$ and set

$$\widetilde{w}_k^{(i)} = \frac{g_k(\mathcal{Z}_k | \mathcal{Z}_{0:k-1}, \widetilde{X}_{0:k}^{(i)}) f_X(\widetilde{X}_k^{(i)} | X_{k-1}^{(i)}, U_{k-1})}{f_X(\widetilde{X}_k^{(i)} | X_{k-1}^{(i)}, U_{k-1})} w_{k-1}^{(i)}.$$

- Normalise weights: $\sum_{i=1}^N \widetilde{w}_k^{(i)} = 1$.

Step 2: *Resampling Step*

- Resample $\left\{ \widetilde{w}_k^{(i)}, \widetilde{X}_{0:k}^{(i)} \right\}_{i=1}^N$ to get $\left\{ w_k^{(i)}, X_{0:k}^{(i)} \right\}_{i=1}^N$.

Since the vehicle transition density is chosen as the proposal density as with FastSLAM 1.0 [6],

$$\widetilde{w}_k^{(i)} = g_k(\mathcal{Z}_k | \mathcal{Z}_{0:k-1}, \widetilde{X}_{0:k}^{(i)}) w_{k-1}^{(i)} \tag{35}$$

which can be evaluated in closed form according to (26) or (27), where,

$$\hat{\mathfrak{m}}_{k|k-1}^{(i)} = \sum_{j=1}^{J_{k|k-1}^{(i)}} \eta_{k|k-1}^{(i,j)} \text{ and } \hat{\mathfrak{m}}_k^{(i)} = \sum_{j=1}^{J_k^{(i)}} \eta_k^{(i,j)}. \tag{36}$$

Note that the incorporation of the measurement conditioned proposal of FastSLAM 2.0 can also be accommodated in this framework. This direction of research focuses on more efficient SMC approximations and is an avenue for further studies.

C. State Estimation and Pseudo-code

As alluded to throughout this paper, in contrast to previous SLAM algorithms, the PHD map representation allows for a natural ability to average feature maps. That is, independent map estimates from N independent trajectory particles can be readily averaged into an expected estimate, even with map estimates of different size and without having to resolve the intra-map feature associations. Consequently, in the case of the RB-PHD-SLAM filter, both the expected vehicle trajectory and feature map can be determined as follows:

Given the posterior set of weighted particles and corresponding map PHDs,

$$\left\{ w_k^{(i)}, X_{0:k}^{(i)}, v_k^{(i)}(m | X_{0:k}^{(i)}) \right\}_{i=1}^N,$$

and $\bar{w} = \sum_{i=1}^N w_k^{(i)}$ then,

$$\hat{X}_{0:k} = \frac{1}{\bar{w}} \sum_{i=1}^N w_k^{(i)} X_{0:k}^{(i)}. \tag{37}$$

As demonstrated previously in section IV-B, the posterior PHD of the map is the expectation of the trajectory-conditioned PHDs and thus,

$$v_k(m | X_{0:k}) = \frac{1}{\bar{w}} \sum_{i=1}^N w_k^{(i)} v_k(m | X_{0:k}^{(i)}). \tag{38}$$

If $\hat{\mathfrak{m}}_k = \int v_k(m | X_{0:k}) dm$, is the mass of the posterior map PHD, the expected map estimate can then be extracted by choosing the $\hat{\mathfrak{m}}_k$ highest local maxima. The pseudo-code for the RB-PHD-SLAM filter and expectation estimator are provided in tables I, II, III and IV. The following section presents the results and analysis of the proposed filter.

TABLE I
RB-PHD-Filter: Prediction

```
Given $\{w_{k-1}^{(i)}, X_{k-1}^{(i)}, v_{k-1}^{(i)}\}_{i=1}^N$, $v_{k-1}^{(i)} = \{\eta_{k-1}^{(i,j)}, \mu_{k-1}^{(i,j)}, P_{k-1}^{(i,j)}\}_{j=1}^{J_{k-1}^{(i)}}$
For $i = 1, \ldots, N$
 Step 1 (Predict pose)
      $\widetilde{X}_k^{(i)} \sim f_X(X_k | X_{0:k-1}^{(i)}, U_{0:k-1}, X_0)$
 Step 2 (Predict map PHD given $\widetilde{X}_k^{(i)}$)
      $l = 0$
      for $j = 1, \ldots, J_{b,k}^{(i)}$ (new Gaussian components)
          $l = l + 1$
          $\eta_{k|k-1}^{(i,l)} = \eta_{b,k}^{(i,j)}$, $\mu_{k|k-1}^{(i,l)} = \mu_{b,k}^{(i,j)}$, $P_{k|k-1}^{(i,l)} = P_{b,k}^{(i,j)}$
      end
      for $j = 1, \ldots, J_{k-1}^{(i)}$ (existing Gaussian components)
          $l = l + 1$
          $\eta_{k|k-1}^{(i,l)} = \eta_{k-1}^{(i,j)}$, $\mu_{k|k-1}^{(i,l)} = \mu_{k-1}^{(i,j)}$, $P_{k|k-1}^{(i,l)} = P_{k-1}^{(i,j)}$
      end
      $J_{k|k-1}^{(i)} = l$, $\hat{\mathfrak{m}}_{k|k-1}^{(i)} = \sum_{j=1}^{J_{k|k-1}^{(i)}} \eta_{k|k-1}^{(i,j)}$
End
```

VI. Results & Analysis

This section presents the results and analysis of the proposed approach using both simulated and experimental datasets. For comparative purposes, the benchmark algorithms used are the classical FastSLAM [6] with Multiple Hypothesis Data association [35] and the Joint Compatibility Branch and Bound (JCBB) EKF [8]. The 'single feature map' trajectory weighting of (27) is adopted for the proposed RB-PHD-SLAM filter, with an implementation using the 'empty map update' of (26) appearing in [11]. While any feature can theoretically be selected to generate the trajectory weighting, in this implementation, that which generates the maximum likelihood amongst all measurements is chosen. A comprehensive study as to the best suited feature selection strategies is left to future work.

TABLE II
RB-PHD-FILTER: MAP UPDATE

```
For $i = 1, \ldots, N$
Step 1 (Compute Update Terms)
    for $j = 1, \ldots, J^{(i)}_{k|k-1}$
        $\hat{z}^{(i,j)} = H_k[X^{(i)}_k \; \mu^{(i,j)}_{k|k-1}]^T$
        $S^{(i,j)}_k = \nabla H_k P^{(i,j)}_{k|k-1} [\nabla H_k]^T + R$
        $K^{(i,j)}_k = P^{(i,j)}_{k|k-1} [\nabla H_k]^T [S^{(i,j)}_k]^{-1}$
        $P^{(i,j)}_{k|k} = [I - K^{(j)}_k \nabla H_k] P^{(i,j)}_{k|k-1}$
    end
Step 2 (Update GMM PHD Components)
    for $j = 1, \ldots, J^{(i)}_{k|k-1}$ (missed detections)
        $\eta^{(i,j)}_k = (1 - P_D)\eta^{(i,j)}_{k|k-1}, \; \mu^{(i,j)}_k = \mu^{(i,j)}_{k|k-1},$
        $P^{(i,j)}_k = P^{(i,j)}_{k|k-1}$
    end
    $l = 0$
    for each $z \in \mathcal{Z}_k$ (detections)
        $l = l + 1$
        for $j = 1, \ldots, J^{(i)}_{k|k-1}$
            $\tau^{(j)} = P_D \eta^{(i,j)}_{k|k-1} \mathcal{N}(z; \hat{z}^{(i,j)}, S^{(i,j)}_k)$
            $\mu^{(lJ^{(i)}_{k|k-1}+j)}_k = \mu^{(i,j)}_{k|k-1} + K^{(i,j)}_k (z - \hat{z}^{(i,j)})$
            $P^{(lJ^{(i)}_{k|k-1}+j)}_k = P^{(i,j)}_{k|k}$
        end
        for $j = 1, \ldots, J^{(i)}_{k|k-1},$
            $\eta^{(lJ^{(i)}_{k|k-1}+j)}_k = \tau^{(j)} / (c(z) + \sum_{m=1}^{J^{(i)}_{k|k-1}} \tau^{(m)})$
        end
    end
    $J^{(i)}_k = (l+1) J^{(i)}_{k|k-1}, \; \hat{\mathfrak{m}}^{(i)}_k = \sum_{j=1}^{J^{(i)}_k} \eta^{(i,j)}_k$
End
```

TABLE III
RB-PHD-FILTER: TRAJECTORY UPDATE

```
Step 1 (trajectory weight update)
  For $i = 1, \ldots, N$
    if (26): $\widetilde{w}^{(i)}_k = \left[c(z)^{|\mathcal{Z}_k|} \exp^{(\hat{\mathfrak{m}}^{(i)}_k - \hat{\mathfrak{m}}^{(i)}_{k|k-1} - \lambda_c)}\right] w^{(i)}_{k-1}$
    if (27): $j = \{j \in [1, \ldots, J^{(i)}_{k|k-1}] | m^{(i,j)} = \bar{m}\}$ then,
      $\widetilde{w}^{(i)}_k = \frac{a}{b} w^{(i)}_{k-1}$ where,
      $a = (1 - P_D)(c(z)^{|\mathcal{Z}_k|}) +$
          $P_D \eta^{(i,j)}_{k|k-1} \Big( \sum_{z \in \mathcal{Z}_k} (c(z)^{|\mathcal{Z}_k|-1}) \mathcal{N}(z; \hat{z}^{(i,j)}, S^{(i,j)}_k) \Big)$
      $b = (c(z)^{|\mathcal{Z}_k|}) \eta^{(i,j)}_k$
  End
Step 2 (Resample, if necessary)
    $\{w^{(i)}_k, X^{(i)}_k, v^{(i)}_k\}_{i=1}^N \sim \{\widetilde{w}^{(i)}_k, \widetilde{X}^{(i)}_k, \widetilde{v}^{(i)}_k\}_{i=1}^N$
```

Current SLAM filters deal with clutter through 'feature management' routines, such as the landmark's quality [5] or a binary Bayes filter [6]. These operations are typically independent of the joint SLAM filter update, whereas the proposed approach unifies feature management, data association and state filtering into a single Bayesian update. While these methods have been used successfully, they generally discard the sensor's detection (P_D) and false alarm (P_{FA}) probabilities and thus can be erroneous when subject to large clutter rates and/or measurement noise. Since the proposed approach assumes knowledge of these probabilities, as seen in (23), a modified feature management routine coined the 'feature existence filter' (see Appendix B), which incorporates both P_D and P_{FA}, is used in the benchmark algorithms.

TABLE IV
RB-PHD-FILTER: EAP ESTIMATOR

```
Given $\{w^{(i)}_k, X^{(i)}_k, v^{(i)}_k\}_{i=1}^N$ and $v^{(i)}_k = \{\eta^{(i,j)}_k, \mu^{(i,j)}_k, P^{(i,j)}_k\}_{j=1}^{J^{(i)}_k}$,
a map merging threshold T, set $v_k = \{\eta^{(j)}_k, \mu^{(j)}_k, P^{(j)}_k\}_{j=1}^{J_k} =$
$\{w^{(i)}_k \eta^{(1,j)}_k, \mu^{(1,j)}_k, P^{(1,j)}_k\}_{j=1}^{J^{(1)}_k}$
Step 1 (the expected vehicle trajectory)
  $\hat{X}_{1:k} = \frac{1}{\bar{w}} \sum_{i=1}^N w^{(i)}_k X^{(i)}_{1:k}$
Step 2 (the expected map PHD, $v_k$)
  set i=2, l=0
  do while$(i <= N)$
    $l = J_k$
    for $j = 1, \ldots, J^{(i)}_k$
      $l = l + 1$
      $\eta^{(l)}_k = w^{(i)}_k \eta^{(i,j)}_k, \mu^{(l)}_k = \mu^{(i,j)}_k, P^{(l)}_k = P^{(i,j)}_k$
    end
    $\mathcal{R} = \{l, \ldots, J_k + J^{(i)}_k\}$
    do while$(|\mathcal{R}| > 0)$(merge map PHDs)
      $l = l + 1$
      $\mathcal{L} = \{r \in \mathcal{R} | (\mu^{(j)}_k - \mu^{(r)}_k)^T (P^{(j)}_k)^{-1} (\mu^{(j)}_k - \mu^{(r)}_k) \leq T\}$
      $\eta^{(l)}_k = \sum_{r \in \mathcal{R}} \eta^{(r)}_k$
      $\mu^{(l)}_k = \frac{1}{\eta^{(l)}_k} \sum_{r \in \mathcal{R}} \eta^{(r)}_k \mu^{(r)}_k$
      $P^{(l)}_k = \frac{1}{\eta^{(l)}_k} \sum_{r \in \mathcal{R}} \eta^{(r)}_k \big(P^{(j)}_k + (\mu^{(l)}_k - \mu^{(r)}_k)(\mu^{(l)}_k - \mu^{(r)}_k)^T\big)$
      $J_k = J_k - |\mathcal{L}| + 1, \mathcal{R} = \mathcal{R} - \mathcal{L}$
    end
    $i = i + 1$
  end
  for $j = 1, \ldots, J_k$ (average weights)
    $\eta^{(j)}_k = \frac{1}{\bar{w}} \eta^{(j)}_k$
  end
Step 3 (the expected map estimate)
  $\hat{\mathcal{M}}_k = \emptyset$
  for $j = 1, \ldots, J_k$
    if $\eta^{(j)}_k > \tau$
      $\hat{\mathcal{M}}_k = [\hat{\mathcal{M}}_k \; \mu^{(j)}_k]$
    end
  end
```

To quantify the map estimation error, a metric must be adopted which jointly evaluates the error in the feature location *and* number estimates. Current methods typically examine the location estimates of a selected number of features and obtain their MSE using ground truth [5]. As such, vector-based error metrics are applied to feature maps and the error in the estimated *number* of features is neglected. While there are several metrics for finite-set-valued estimation error, that of [13] has been demonstrated to be most suitable [10], [11]. Briefly, the metric optimally assigns each feature estimate to its ground truth through the Hungarian assignment algorithm and evaluates an error distance, while penalising for under/over estimating the number of features. Based on a 2^{nd}-order Wasserstein construction, if $|\mathcal{M}_k| > |\hat{\mathcal{M}}_k|$, the feature map estimation error is given by,

$$\bar{d}^{(c)}(\hat{\mathcal{M}}_k, \mathcal{M}_k) := \Bigg(\frac{1}{|\mathcal{M}_k|} \Bigg(\min_{j \in perm(\mathcal{M}_k)} \sum_{i=1}^{|\hat{\mathcal{M}}_k|} d^{(c)}(\hat{m}^i, m^{j(i)})^2 + c^2(|\mathcal{M}_k| - |\hat{\mathcal{M}}_k|) \Bigg) \Bigg)^{1/2} \tag{39}$$

where, $d^{(c)}(\hat{m}^i, m^{j(i)}) = \min(c, ||\hat{m}^i - m^{j(i)}||)$ is the minimum of the cut-off parameter, c, and the Euclidean distance between the estimated feature location, $\hat{m}^i$ and the true feature location $m^{j(i)}$. If $|\mathcal{M}_k| < |\hat{\mathcal{M}}_k|$, the metric is obtained through $\bar{d}^{(c)}(\mathcal{M}_k, \hat{\mathcal{M}}_k)$. To incorporate oriented features for instance, other vector distances such as a Mahalanobis distance could be used. It is important to note that the error distance of (39) is mathematically consistent, in that the metric satisfies the necessary axioms and enjoys most of the properties of a Euclidean distance. Furthermore the metric topology is the same as the topology of the underlying space of set-valued maps [13]. In the following subsections, this metric along with the estimated trajectory RMSE and graphical comparisons are used to demonstrate the merits of the RB-PHD-SLAM filter.

A. *Simulated Dataset*

Simulated trials were carried out, due to the ease of generating known ground truth (trajectories and maps) for estimation error evaluation. The parameters for the simulated trials were: velocity input standard deviation (std.) of $2m/s$, steering input std. of 5^o, range measurement std. of $1m$ and bearing measurement std. of 2^o, $P_D = 0.95$, $\lambda_c = 20$, using a sensor with 10m maximum range and a 360^o field of view. The feature existence probability threshold is set at 0.5, and a 95% gate is used throughout. For each SLAM filter, 50 Monte Carlo (MC) trials were carried out in which all methods received identical sequences of control inputs and measurements. The RB based filters used 50 trajectory particles each, while for MHT-FastSLAM a maximum limit of 2000 particles (number of hypotheses considered prior to resampling) was used.

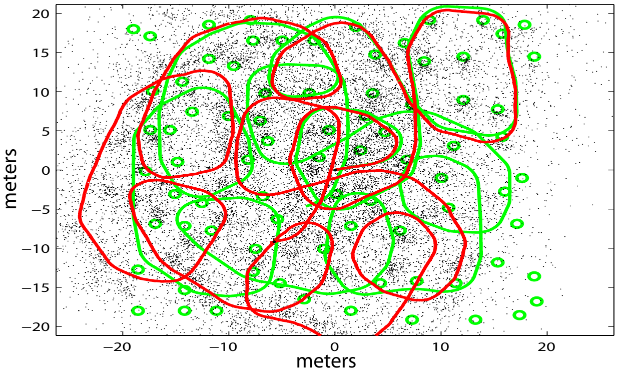

Fig. 4. *The simulated environment showing point features (green circles) and true vehicle trajectory (green line). A sample measurement history plotted from a sample noisy trajectory (red line) is also shown (black points).*

Figure 4 shows a sample of the raw input data used in the trials, superimposed onto the ground truth feature map and path. A comparison of the average trajectory estimation errors for all three filters is then presented in Figure 5. In terms of the estimated trajectory, the first order RB-PHD-SLAM algorithm can be seen to outperform the vector based FastSLAM with robust data association, but does not quite achieve the estimation accuracy of JCBB-EKFSLAM. This is primarily due to the fact that JCBB is very conservative in its choice of measurement-feature associations (jointly compatible constraint) resulting in very few false association pairs influencing the trajectory estimation. However, later results in Figures 6, 7 and 9 highlight the drawbacks of achieving such impressive localisation results.

In terms of the map estimation component of each SLAM algorithm, Figure 6 depicts both the true and estimated number of features as the vehicle explores the map, with the proposed RB-PHD-SLAM approach seen to closely track the true number of features in the explored map. Erroneous associations for the MHT-FastSLAM approach result in excessive feature declarations, while the conservative (only including those which are jointly compatible) association decisions of JCBB-EKF SLAM reduces the number of correct associations. Since vector based feature management routines are typically dependant on the data association decisions, this dramatically influences the map estimation error.

Incorporating the estimation error in both the number and location of features in the map, Figure 7 plots the map error distance of (39) for each approach. Note that in order to generate this result, the vector based maps of FastSLAM and JCBB-EKFSLAM are temporarily 'assumed' to be sets. The proposed method can be seen to report the least mapping error due it is robust ability to jointly incorporate uncertainty in feature locations and numbers, while erroneous feature estimates contribute to increased mapping error for the vector based approaches. A qualitative depiction of the posterior estimates is provided in Figure 8, demonstrating the usefulness of the RFS-SLAM framework and the proposed RB-PHD-SLAM filter.

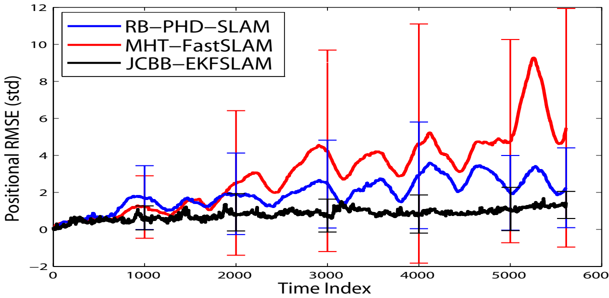

Fig. 5. *The mean and standard deviation of the trajectory estimates from each filter over 50 MC runs versus time.*

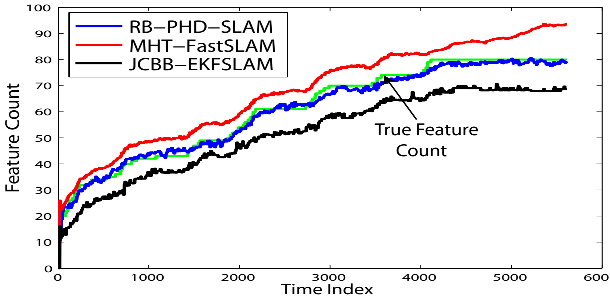

Fig. 6. *The average estimated number of features in the map for each filter versus time, compared to the ground truth number of features in the explored map $\mathcal{M}_k$. The feature number estimate of RB-PHD-SLAM can be seen to closely track that of the ground truth.*

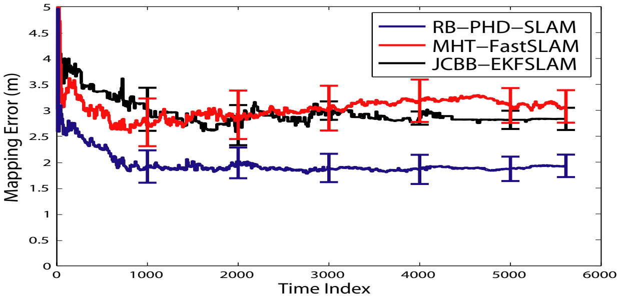

Fig. 7. *A comparative plot of the mean and standard deviation of the map estimation error for each filter vs. time. At any given time, for the ideal case, the mapping error from (39) wrt. the explored map is zero.*

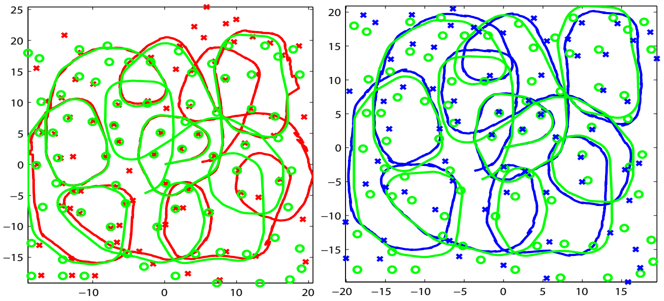

Fig. 8. *Comparisons of the posterior SLAM estimates from MHT-FastSLAM (left, red) and the proposed RB-PHD-SLAM (right, blue). The ground truth trajectory and map are represented by the green line and circles respectively. The RB-PHD-SLAM filter demonstrates its robustness and accuracy given high clutter and data association ambiguity.*

B. Complexity and Computation Time

As seen from section V, the computational complexity of RB-PHD-SLAM is, $\mathcal{O}(\mathfrak{m}_k \mathfrak{z}_k N)$ i.e. linear in the number of features (in the FoV), linear in the number of measurements and linear in the number of trajectory particles. Furthermore, in contrast to DA based methods, the proposed approach admits numerous computational enhancements, since the map PHD update of (23) can be segmented, executed in parallel and subsequently fused for state estimation. This is in contrast to DA based approaches which are scalable.

For a single thread implementation (without the Tree-based enhancements [6]), Figure 9 shows that the computation time is comparable with that of the MHT-FastSLAM algorithm, both of which are less expensive than JCBB-EKF SLAM as its hypothesis tree grows in the presence of high clutter.

C. Experimental Dataset

This section discusses the filter's performance in a surface-based marine environment, using an X-band radar mounted on a powerboat. In order to maximize the detection of all sea surface point features (comprising boats, buoys, etc.), a low detection threshold is required, which subsequently increases the clutter rate. GPS data is available for measuring the ground truth trajectory, while sea charts and data from surrounding vessels' Automatic Identification Systems provide the feature map ground truth. The test site is off the Southern coast of Singapore, as shown in Figure 10, where the boat was driven in looping trajectory of 13Km. Adaptive thresholding methods were applied to extract relative point measurements from the radar data [36]. The maximum range of the radar, logging at 0.5Hz, was limited to 1Km. While heading measurements were available via a low grade on-board single axis gyroscope, due to the lack of doppler velocity logs, the speed was estimated at 8 knots (4.1 m/s).

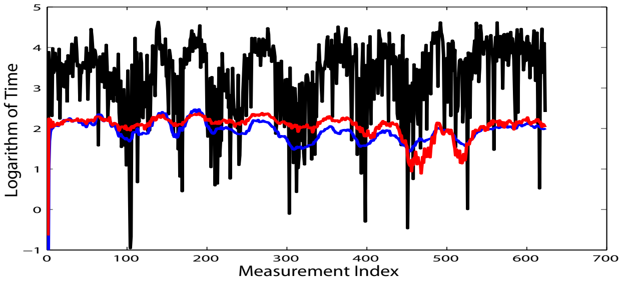

Fig. 9. *A comparison of the computation time per measurement update for RB-PHD-SLAM (blue), MHT-FastSLAM (red) and JCBB-EKFSLAM (black).*

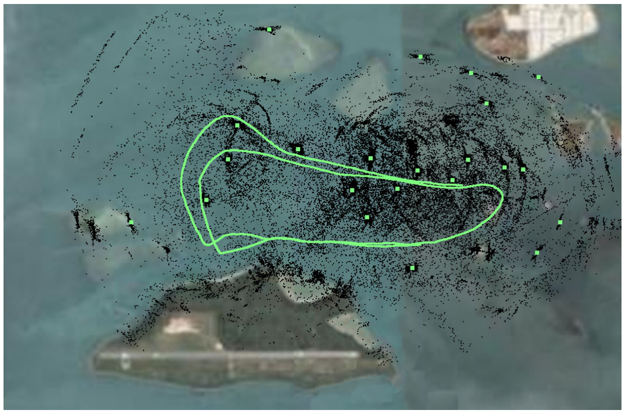

Fig. 10. *Overview of the test site (1°13′ N,103°43′ E), showing the GPS trajectory (green line) and GPS co-ordinates (green dots) of the point feature map. The point feature measurement history is also provided (black dots).*

Figure 11 compares the posterior SLAM estimates from MHT-FastSLAM and RB-PHD-SLAM, with Figure 12 comparing the estimated map sizes. The proposed approach can be seen to generate more accurate localisation and feature number estimates, however it can also be seen that some feature estimates are mis-placed in comparison to the ground truth feature map. The framework is still demonstrated to be useful for high clutter feature-based SLAM applications.

D. Future Directions

The RFS-SLAM framework proposed in this paper offers numerous extensions and other solutions. For instance, the Poisson assumption of the PHD approach can be relaxed via the Cardinalised PHD construct [37] and the multiBernoulli recursion [38]. As with the PHD approximation, the trajectory conditioned measurement likelihood can be calculated exactly

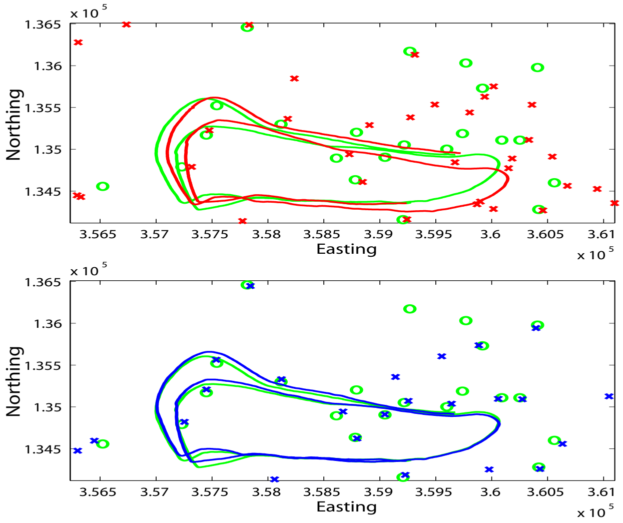

Fig. 11. *Top: The posterior SLAM estimate (red) from MHT-FastSLAM and Bottom: The posterior SLAM estimate (blue) from RB-PHD-SLAM, in comparison to the ground truth (green).*

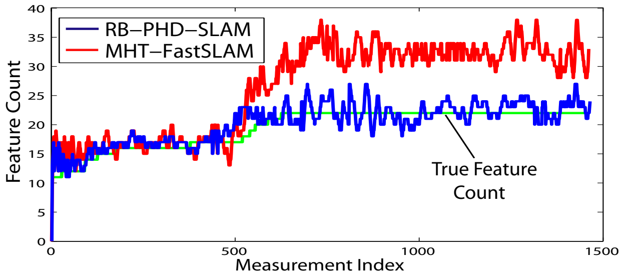

Fig. 12. *Comparison of the number of estimated features for each approach. The noisy estimates are likely due to deviations from the Poisson clutter assumption in places.*

for each representation. The proposed RFS framework may also be modified maximum likelihood (ML) approaches [39].

1) RB-CPHD-SLAM: Let the density of the RFS map of (20) be approximated by an iid cluster RFS, which is completely characterised by its cardinality distribution, ρ_k, and PHD, v_k, and where $\mathbb{E}[\rho_k] = \int v_k(m)dm$. The trajectory conditioned map recursion of (15) may then be approximated by a CPHD filter [37], and the trajectory conditioned measurement likelihood of (25) can be evaluated as in [11]. Given that the CPHD filter propagates the *distribution* of the number of features as opposed to just its mean (for the PHD approach of this paper), it is anticipated that the map, and subsequently the trajectory, estimates from RB-CPHD-SLAM would be remarkably improved in comparison to RB-PHD-SLAM.

2) RB-MeMBer-SLAM: A multi-Bernoulli RFS is simply a set of Bernoulli RFSs mentioned previously in section II-B, and is completely described by the multi-Bernoulli parameter set $\{(\epsilon_k^{(i)}, \pi_k^{(i)})\}_{i=1}^{\mathfrak{m}_k}$. As with RB-CPHD-SLAM, if the RFS map density of (15) is approximated by a multi-Bernoulli RFS, the trajectory conditioned map recursion of (15) may be approximated by a MeMBer filter [38], and again the trajectory conditioned measurement likelihood of (25) can be evaluated as in [11].

Differing from RB-PHD-SLAM and RB-CPHD-SLAM, RB-MeMBer-SLAM propagates a set of features and their corresponding existence probabilities. Using a Bernoulli RFS to represent each feature allows for the joint encapsulation of its existence probability and location in a single pdf, thus enhancing existing approaches in SLAM, which typically model the existence probability and location as separate independent entities [5], [6]. It is expected that RB-MeMBer-SLAM would perform well in the presence of highly non-linear process and/or measurement models.

3) ML-RFS-SLAM: In contrast to the above-mentioned RBPF solutions, the proposed RFS-SLAM framework can also be adapted to the popular maximum likelihood approaches, which formulate SLAM as a non-linear stochastic optimisation problem [39], [40]. Recently, methods of estimating the parameters of the measurement likelihood from the PHD filter using SMC have been proposed [41]. Assuming a finite-set measurement and state, the gradient of the likelihood function was estimated and used to determine the ML estimate of the unknown measurement parameters such as the clutter rate. Thus the RFS-SLAM framework can also admit ML type vehicle trajectory estimation, such as in that of [40]. By formulating a suitable likelihood function and estimating the feature map using the proposed PHD/CPHD/MeMBer methods, gradients could be evaluated to extract the ML vehicle trajectory.

VII. Conclusion

This paper establishes that, from a fundamental estimation viewpoint, a feature-based map is a finite set and subsequently presented a Bayesian filtering formulation as well as a tractable solution for the feature-based SLAM problem. The filter jointly propagates and estimates the vehicle trajectory, number of features in the map as well as their individual locations in the presence of data association uncertainty and clutter. The key to the approach is to adopt the natural finite-set representation of the map and to use the tools of finite-set-statistics to cast the problem into the Bayesian paradigm. It is shown that this Bayesian formulation admits a number of optimal Bayes estimators for SLAM. The finite set representation of the map admits the notion of expected map in the form of a PHD or intensity function. The PHD construct can also be interpreted in terms of occupancy maps. A Rao-Blackwellised implementation of the filter was proposed, in which the PHD of the map was propagated using a Gaussian mixture PHD filter, and a particle filter propagated the vehicle trajectory density.

Analysis was carried out both in a simulated environment through Monte Carlo trials and an outdoor SLAM experimental dataset based on an X-band marine radar sensor. Results demonstrated the robustness of the proposed filter, particulary in the presence of large data association uncertainty and clutter, illustrating the merits of adopting an RFS approach to SLAM. Furthermore, the framework admits numerous avenues of future research into maximum likelihood approaches or enhancements via the CPHD and MeMBer filters, which are expected to improve the performance and increase robustness to clutter, data association difficulty and highly non-linear process/measurement models.

VIII. Acknowledgements

This research is funded in part by the Singapore National Research Foundation through the Singapore-MIT Alliance for Research and Technology CENSAM. The second author is supported in part by discovery grant DP0880553 awarded by the Australian Research Council. The fourth author is supported by the discovery grant DP0989007, from the Australian Research Council and is also a recipient of an Australian Postdoctoral Fellowship. We also thank the reviewers for their valuable comments.

References

[1] R. Smith, M. Self, and P. Cheeseman. Estimating uncertain spatial relationships in robotics. *Autonomous Robot Vehicles*, 1990.

[2] S. Thrun. Particle filter in robotics. In *Uncertainty in AI (UAI)*, 2002.

[3] D. Makarsov and H.F. Durrant-Whyte. Mobile vehicle navigation in unknown environments: a multiple hypothesis approach. *IEE Proceedings of Contr. Theory Applict.*, vol. 142, July 1995.

[4] J. Guivant, E. Nebot, and S. Baiker. Autonomous navigation and map building using laser range sensors in outdoor applications. *Journal of Robotic Systems*, 17(10):565–583, October 2000.

[5] G. Dissanayake, P. Newman, H.F. Durrant-Whyte, S. Clark, and M. Csorba. A solution to the simultaneous localization and map building (SLAM) problem. *IEEE Transactions on Robotic and Automation*, 17(3):229–241, June 2001.

[6] M. Montemerlo, S. Thrun, and B. Siciliano. *FastSLAM: A Scalable Method for the Simultaneous Localization and Mapping Problem in Robotics*. Springer, 2007.

[7] H.F. Durrant-Whyte and T. Bailey. Simultaneous localization and mapping: Part I. *IEEE Robotics and Automation Magazine*, 13(2):99–110, June 2006.

[8] J. Niera and J.D. Tardos. Data association in stochastic mapping using the joint compatibility test. *IEEE Transactions on Robotics and Automation*, 17(6):890–897, December 2001.

[9] J. Mullane, B.N. Vo, M. Adams, and W.S. Wijesoma. A random set formulation for bayesian SLAM. In *proceedings of the IEEE/RSJ International Conference on Intelligent Robots and Systems*, France, September 2008.

[10] J. Mullane, B.N. Vo, M. Adams, and W.S. Wijesoma. A random set approach to SLAM. In *proceedings of the IEEE International Conference on Robotics and Automation (ICRA) workshop on Visual Mapping and Navigation in Outdoor Environments*, Japan, May 2009.

[11] J. Mullane, B.N. Vo, and M. Adams. Rao-blackwellised PHD SLAM. In *proceedings of the IEEE International Conference on Robotics and Automation (ICRA)*, Alaska, USA, May 2010.

[12] J.R. Hoffman and R. Mahler. Multi-target miss distance via optimal assignment. *IEEE Transactions on Systems, Man and Cybernetics*, 34(3):327–336, May 2004.

[13] D. Schuhmacher, B.T. Vo, and B.N. Vo. A consistent metric for performance evaluation of multi-object filters. *IEEE Transactions on Signal Processing*, 86(8):3447–3457, 2008.

[14] G. Grisetti, C. Stachniss, and W. Burgard. Improved techniques for grid mapping with rao-blackwellized particle filters. *IEEE Transactions on Robotics*, 23(1):34–45, February 2007.

[15] Y. Rachlin, J.M. Dolan, and P. Khosla. Efficient mapping through exploitation of spatial dependencies. In *proceedings of the IEEE/RSJ International Conference on Intelligent Robots and Systems (IROS)*, Alberta, Canada, August 2005.

[16] R. Mahler. Multi-target bayes filtering via first-order multi-target moments. *IEEE Transactions on AES*, 4(39):1152–1178, October 2003.

[17] R. Mahler. *Statistical Multisource Multitarget Information Fusion*. Artech House, 2007.

[18] B.N. Vo, S. Singh, and A. Doucet. Sequential monte carlo methods for multi-target filtering with random finite sets. *IEEE Transactions on Aerospace and Electronic Systems*, 41(4):1224–1245, October 2005.

[19] M. Tobias and A. Lanterman. A probability hypothesis density based multitarget tracking with multiple bistatic range and doppler observations. *IEE Radar Sonar and Navigation*, 152(3):195–205, 2005.

[20] T. Wood. Random finite set theory for tracking. http://people.maths.ox.ac.uk/∼woodtm/rfs_overview.pdf, February 2010.

[21] B.T. Vo. *Random finite sets in multi-object filtering*. PhD thesis.

[22] R. Mahler. Implementation and application of PHD/CPHD filters. In *Int'l Conf. on Information Fusion*, Seattle, WA, 2009.

[23] S. Kay. *Fundamentals of Statistical Signal Processing, Vol I - Estimation Theory*. Prentice Hall, 1998.

[24] C. Roberts. *The Bayesian Choice: From Decision-Theoretic Foundations to Computational Implementation*. Springer, 2001.

[25] R. Murphy. Bayesian map learning in dynamic environments. In *Proc. Conf. Neural Inf. Process. Syst.*, pages 1015–1021, Colorado, 1999.

[26] P. Del Moral and J. Jacod. *The Monte-Carlo Method for filtering with discrete time observations. Central Limit Theorems.* The Fields Institute Communications American Mathematical Society, 2002.

[27] D. Crisan and A. Doucet. A survey of convergence results on particle filtering methods for practitioners. *IEEE Transactions on Signal Processing*, 50(3):736–746, March 2002.

[28] D.J. Daley and D. Vere-Jones. *An Introduction to the Theory of Point Processes*. Springer, NY, USA, 2002.

[29] D. Stoyan, W.S Kendall, and J. Mecke. *Stochastic Geometry and Its Applications*. John Wiley and Sons, Inc, New York, second edition, 1995.

[30] A. Brooks and T. Bailey. HybridSLAM: Combining FastSLAM and EKF-SLAM for reliable mapping. In *the Eighth International Workshop on the Algorithmic Foundations of Robotics*, Mexico, December 2008.

[31] O. Erdinc, P. Willett, and Y. Bar-Shalom. The bin-occupancy filter and its connection to the PHD filters. *IEEE Transactions on Signal Processing*, 57(11):4232–4246, November 2009.

[32] B. Kaylan, K.W. Lee, and W.S. Wijesoma. FISST-SLAM: Finite set statistical approach to simultaneous localization and mapping. *International Journal of Robotics Research*, 29(10):1251–1262, September 2010.

[33] H.F. Durrant-Whyte, S. Majumder, M. de Battista, and S. Scheding. A bayesian algorithm for simultaneous localisation and map building. In *The Tenth International Symposium of Robotics Research (ISRR)*, Victoria, Australia, 2001.

[34] B.N. Vo and W.K. Ma. The gaussian mixture probability hypothesis density filter. *IEEE Transactions on Signal Processing*, 54(11):4091–4104, November 2006.

[35] J. Nieto, J. Guivant, E. Nebot, and S. Thrun. Real time data association for fastslam. In *IEEE Internationlal Conference on Robotics and Automation*, volume 1, pages 412–418, September 2003.

[36] J. Mullane, S. Keller, A. Rao, M. Adams, A. Yeo, F. Hover, and N. Patrikalakis. X-band radar based SLAM in singapores off-shore environment. In *proceedings of the 11th IEEE ICARCV*, Singapore, December 2010.

[37] B.T. Vo, B.N. Vo, and A. Cantoni. Analytic implementations of the cardinalized probability hypothesis density filter. *IEEE Transactions on Signal Processing*, 55(7):3553–3567, July 2007.

[38] B.T. Vo, B.N. Vo, and A. Cantoni. The cardinality balanced multi-target multi-bernoulli and its implementations. *IEEE Transactions on Signal Processing*, 57(2):409–423, February 2009.

[39] M. Kaess, A. Ranganathan, and F. Dellaert. iSAM: Incremental smoothing and mapping. *IEEE Transactions on Robotics*, 24(6):1365–1378, December 2008.

[40] E. Olson, J. Leonard, and S. Teller. Fast iterative optimization of pose graphs with poor initial estimates. In *IEEE Internationlal Conference on Robotics and Automation*, May 2006.

[41] S.S. Singh, N. Whiteleyy, and S. Godsill. An approximate likelihood method for estimating the static parameters in multi-target tracking models. Technical report, Cambridge, UK., 2009.

Appendix A
Derivation of $g_k(\mathcal{Z}_k|\mathcal{Z}_{0:k-1}, X_{0:k})$ for the RB-PHD-SLAM Filter

Recall (15),

$$p_k(\mathcal{M}_k|X_{0:k}) = \frac{g_k(\mathcal{Z}_k|\mathcal{M}_k, X_k)p_{k|k-1}(\mathcal{M}_k|X_{0:k})}{g_k(\mathcal{Z}_k|\mathcal{Z}_{0:k-1}, X_{0:k})}$$

and the Poisson RFS approximations,

$$p_{k|k-1}(\mathcal{M}_k|X_{0:k}) \approx \frac{\prod\limits_{m\in\mathcal{M}_k} v_{k|k-1}(m|X_{0:k})}{\exp\left(\int v_{k|k-1}(m|X_{0:k})dm\right)},$$

$$p_k(\mathcal{M}_k|X_{0:k}) \approx \frac{\prod_{m\in\mathcal{M}_k} v_k(m|X_{0:k})}{\exp\left(\int v_k(m|X_{0:k})dm\right)}.$$

Rearranging, and assigning $\mathcal{M}_k = \emptyset$ gives,

$$g_k(\mathcal{Z}_k|\mathcal{Z}_{0:k-1}, X_{0:k}) = g_k(\mathcal{Z}_k|\emptyset, X_k) \times \frac{\prod_{m\in\mathcal{M}_k} v_{k|k-1}(m|X_{0:k})}{\prod_{m\in\mathcal{M}_k} v_k(m|X_{0:k})} \times \frac{\exp\left(\int v_k(m|X_{0:k})dm\right)}{\exp\left(\int v_{k|k-1}(m|X_{0:k})dm\right)}$$

Since, $\mathcal{M}_k = \emptyset$, the empty set measurement likelihood is that of the clutter RFS (Poisson),

$$g_k(\mathcal{Z}_k|\emptyset, X_k) = \frac{\prod_{z\in\mathcal{Z}_k} c_k(z|X_k)}{\exp(\int c_k(z|X_k)dz)}.$$

Both $\prod_{m\in\mathcal{M}_k} v_{k|k-1}(m|X_{0:k})$ and $\prod_{m\in\mathcal{M}_k} v_k(m|X_{0:k})$ are empty, implying their product is 1, $\hat{\mathfrak{m}}_{k|k-1} = \int v_{k|k-1}(m|X_{0:k})dm$ and $\hat{\mathfrak{m}}_k = \int v_k(m|X_{0:k})dm$, giving,

$$g_k(\mathcal{Z}_k|\mathcal{Z}_{0:k-1}, X_{0:k}) = \prod_{z\in\mathcal{Z}_k} c_k(z|X_k)\times \exp\left(\hat{\mathfrak{m}}_k - \hat{\mathfrak{m}}_{k|k-1} - \int c_k(z|X_k)dz\right).$$

Note that while for the empty map choice, the likelihood $g_k(\mathcal{Z}_k|\mathcal{Z}_{0:k-1}, X_{0:k})$ does not contain a measurement likelihood term, $g_k(\mathcal{Z}_k|\mathcal{M}_k, X_k)$, the history of measurements and trajectories are incorporated into the predicted and updated intensity terms, whose integrals appear as the terms $\hat{\mathfrak{m}}_{k|k-1}$ and $\hat{\mathfrak{m}}_k$ respectively.

Appendix B
FastSLAM Feature Management

This appendix outlines the feature management routine developed for the benchmark filters, incorporating the detection and false alarm probabilities for a fair comparison with the RB-PHD-SLAM filter. As with standard approaches [5], tentative new features are declared for unassociated measurements. The 'existence probability' of each feature, $P^{(j)}_{E,k}$, given a 95% confidence gate and prior existence probability of $P^{(j)}_{E,k-1}$, then evolves through a binary Bayes filter according to the routine of table V. This ad-hoc but effective routine enhances the robustness of standard SLAM feature management when exposed to high clutter rates. Thus both the benchmark and proposed approach receive the same information for each filter loop.

John Mullane received the B.E.E degree (with first-class hons.) in electrical and electronic engineering from University College Cork, Ireland in 2002, and Ph.D degree from Nanyang Technological University (NTU), Singapore in 2009. He is currently a Postdoctoral Research Fellow in the department of electrical and electronic engineering at NTU as part of the Singapore-MIT Alliance for Research and Technology. His research interests include radar signal processing, probabilistic mapping and stochastic mobile robotics.

TABLE V
THE FEATURE EXISTENCE FILTER

Step 1: (Obtain association details within FoV)

$$\bar{J} = \{j \in M_k | m^j \in \text{FoV} \ \&\ m^j \text{ not associated.}\}$$

$$J = \{j \in M_k | m^j \in \text{FoV} \ \&\ m^j \text{ associated.}\}$$

Step 2: (Calculate hit, miss and association probabilities)

$$P^{(\bar{J})}_{miss} = (1 - P_D) \times P^{(\bar{J})}_{E,k-1} + P_D \times 0.05 \times P^{(\bar{J})}_{E,k-1}$$

$$P^{(J)}_{hit} = P_D \times P^{(J)}_{assoc} P^{(J)}_{E,k-1}$$

$$P^{(J)}_{assoc} = \frac{1}{2\pi}|S_k|^{-1/2} \exp(-\frac{1}{2} \upsilon S_k^{-1} \upsilon^T)$$

Step 3: (Update Existence probabilities)

$$P^{(\bar{J})}_{E,k} = \frac{P^{(\bar{J})}_{miss}}{P^{(\bar{J})}_{miss} + (1 - P_{FA})(1 - P^{(\bar{J})}_{E,k-1})}$$

$$P^{(J)}_{E,k} = \frac{P^{(J)}_{hit}}{P^{(J)}_{hit} + P_{FA}(1 - P^{(J)}_{E,k-1})}$$

Ba-Ngu Vo received his Bachelor degrees jointly in Science and Electrical Engineering with first class honours at the University of Western Australia in 1994, and PhD at Curtin University of Technology in 1997. He had held various research positions before joining the department of Electrical and Electronic Engineering at the University of Melbourne in 2000. Currently he is Winthrop Professor and Chair of Signal Processing in the School of Electrical Electronic and Computer Engineering at the University of Western Australia. Dr. Vo is a recipient of the Australian Research Council's inaugural Future Fellowship. His research interests are Signal Processing, Systems Theory and Stochastic Geometry with emphasis on target tracking, robotics and computer vision.

Martin Adams received the degree in engineering science and the D.Phil. degree from the University of Oxford, Oxford, U.K., in 1988 and 1992, respectively. He held positions in the Swiss Federal Institute of Technology and the European Semiconductor Equipment Centre, before joining Nanyang Technological University, Singapore in 2000. He is currently a Professor at the Department of Electrical Engineering and a member of the Advanced Mining Technology Centre (AMTC), University of Chile. His research interests include stochastic estimation and signal processing with applications in autonomous robot navigation, sensing and control.

Ba-Tuong Vo received the B.Sc. degree in applied mathematics and B.E. degree in electrical and electronic engineering (with first-class honors) in 2004, and the Ph.D. degree in engineering (with Distinction) in 2008, all from the University of Western Australia, Crawley. He is currently an Assistant Professor and Australian Postdoctoral Fellow in the School of Electrical, Electronic and Computer Engineering at the University of Western Australia. His primary research interests are in point process theory, filtering and estimation, and multiple object filtering.